Metabolic engineering of *Corynebacterium glutamicum* for production of *scyllo*-inositol, a drug candidate against Alzheimer's disease

Paul Ramp, Alexander Lehnert, Susanna Matamouros, Astrid Wirtz, Meike Baumgart, Michael Bott[#]

IBG-1: Biotechnology, Institute of Bio- and Geosciences, Forschungszentrum Jülich, Jülich, Germany

[#]Corresponding author: m.bott@fz-juelich.de

Highlights

- *C. glutamicum* has the natural potential to synthesize *scyllo*-inositol
- Cg0204 and Cg0207 catalyze the conversion of *myo*-inositol to *scyllo*-inositol
- Deletion of cg3389-cg3392 is crucial for efficient *scyllo*-inositol production
- Complete conversion of *myo*-inositol to *scyllo*-inositol in BHI medium
- Engineered *C. glutamicum* produced 4.4 g *scyllo*-inositol from 20 g sucrose

Graphical abstract

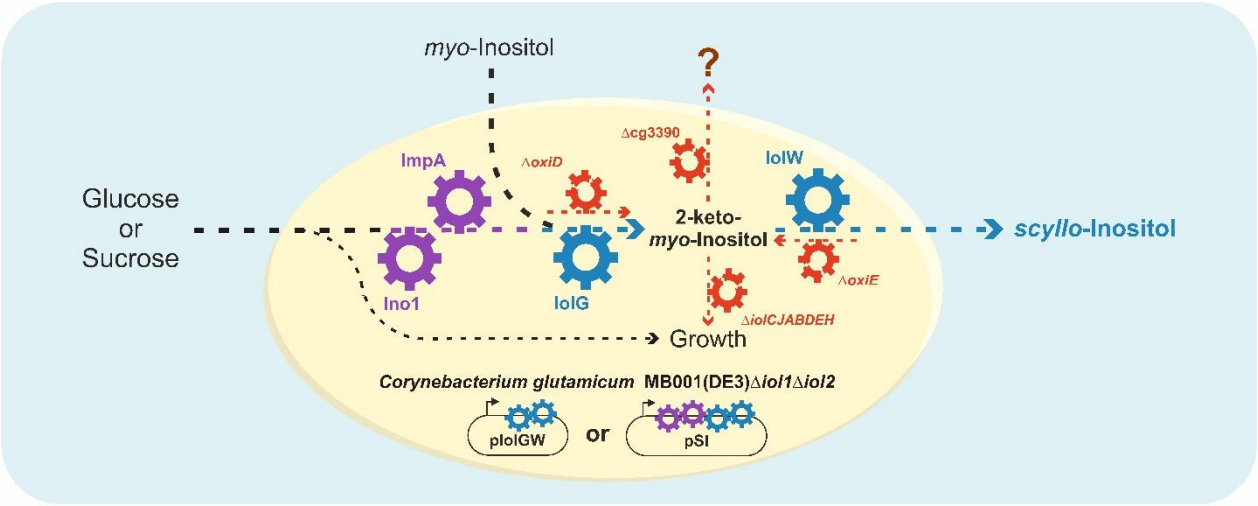

Abstract

Scyllo-inositol has been identified as a potential drug for the treatment of Alzheimer's disease. Therefore, cost-efficient processes for the production of this compound are desirable. In this study, we analyzed and engineered *Corynebacterium glutamicum* with the aim to develop competitive *scyllo*-inositol producer strains. Initial studies revealed that *C. glutamicum* naturally produces *scyllo*-inositol when cultured with *myo*-inositol as carbon source. The conversion involves NAD^+-dependent oxidation of *myo*-inositol to 2-keto-*myo*-inositol followed by NADPH-dependent reduction to *scyllo*-inositol. Use of *myo*-inositol for biomass formation was prevented by deletion of a cluster of 16 genes involved in *myo*-inositol catabolism (strain MB001(DE3)Δ*iol1*). Deletion of second cluster of four genes (*oxiC-cg3390-oxiD-oxiE*) related to inositol metabolism prevented conversion of 2-keto-*myo*-inositol to undesired products causing brown coloration (strain MB001(DE3)Δ*iol1*Δ*iol2*). The two chassis strains were used for plasmid-based overproduction of *myo*-inositol dehydrogenase (IolG) and *scyllo*-inositol dehydrogenase (IolW). In BHI medium containing glucose and *myo*-inositol, a complete conversion of the consumed *myo*-inositol into *scyllo*-inositol was achieved with the Δ*iol1*Δ*iol2* strain. To enable *scyllo*-inositol production from cheap carbon sources, *myo*-inositol 1-phosphate synthase (Ino1) and *myo*-inositol 1-phosphatase (ImpA), which convert glucose 6-phosphate into *myo*-inositol, were overproduced in addition to IolG and IolW using plasmid pSI. Strain MB001(DE3)Δ*iol1*Δ*iol2* (pSI) produced 1.8 g/L *scyllo*-inositol from 20 g/L glucose and even 4.4 g/L *scyllo*-inositol from 20 g/L sucrose within 72 h. Our results demonstrate that *C. glutamicum* is an attractive host for biotechnological production of *scyllo*-inositol and potentially further *myo*-inositol-derived products.

Keywords: *Corynebacterium glutamicum*; metabolic engineering;, *myo*-inositol; *scyllo*-inositol; sucrose; Alzheimer's disease

1. Introduction

Scyllo-inositol, one of nine structural isomers of inositol (1,2,3,4,5,6-cyclohexanehexol), is under study as a promising therapeutic agent for Alzheimer's disease, because of its inhibitory effect on amyloid β protein (Aβ) aggregation and reduction of cerebral Aβ pathology (Fenili et al., 2007; McLaurin et al., 2006; Salloway et al., 2011; Townsend et al., 2006). Therefore, an efficient process for *scyllo*-inositol production is desirable. Although chemical production has been described (Sarmah and Shashldhar, 2003), a biotechnological route might be more promising, as it can start from cheaper precursors such as glucose, avoids the use of hazardous chemicals and high temperatures, and may allow higher yields (Li et al., 2021; Wenda et al., 2011). A pathway for epimerization of *myo*-inositol to *scyllo*-inositol was first proposed using extracts of the fat body of the desert locust *Schistocerca gregaria*, which involved the initial oxidation of *myo*-inositol with NAD^+ to 2-keto-*myo*-inositol (*myo*-inosose) followed by an NADPH-dependent reduction of 2-keto-*myo*-inositol to *scyllo*-inositol (Candy, 1967). The formation of the intermediate 2-keto-*myo*-inositol in this two-step process was confirmed by labeling studies using cells of *Streptomyces griseus* (Horner and Thaker, 1968).

In the past years, several studies were dedicated to the production of *scyllo*-inositol with *Bacillus subtilis*, which is naturally able to catabolize *myo*-inositol (Yoshida et al., 1997). The first step in the degradation pathway is the oxidation of *myo*-inositol to 2-keto-*myo*-inositol by the dehydrogenase IolG, followed by dehydration to 3D-(3,5/4)-trihydroxycyclohexane-1,2-dione (THcHDO) by IolE (Yoshida et al., 2004). This intermediate is converted in subsequent steps to dihydroxyacetone phosphate, acetyl-CoA and CO_2 (Yoshida et al., 2008). Besides *myo*-inositol, *B. subtilis* can also grow with *scyllo*-inositol as sole carbon source and two *scyllo*-inositol dehydrogenases were identified, IolX and IolW (Morinaga et al., 2010). IolX was shown to be essential for growth with *scyllo*-inositol and to catalyze the NAD^+-dependent oxidation of *scyllo*-inositol to 2-keto-*myo*-inositol, which then is degraded via the same pathway used for *myo*-inositol. IolW was dispensable for growth on *scyllo*-inositol and

preferably catalyzed the NADPH-dependent reduction of 2-keto-*myo*-inositol to *scyllo*-inositol (Morinaga et al., 2010). Based on this knowledge a *B. subtilis* strain was constructed that allowed bioconversion of 10 g/L *myo*-inositol to about 4 g/L *scyllo*-inositol (Yamaoka et al., 2011). An improved strain enabled complete conversion of 10 g/L *myo*-inositol into *scyllo*-inositol within 48 h (Tanaka et al., 2013). In a further study, an increase of the Bacto soytone concentration in the medium allowed conversion of 50 g/L *myo*-inositol into 27.6 g/L *scyllo*-inositol (Tanaka et al., 2017). Most recently, further *B. subtilis* strains were constructed that allowed production of 2 g/L *scyllo*-inositol from 20 g/L glucose (Michon et al., 2020). These strains contained *myo*-inositol phosphate synthase from *Mycobacterium tuberculosis*, which converts glucose 6-phosphate to L-*myo*-inositol 1-phosphate, which is then dephosphorylated to *myo*-inositol by the intrinsic inositol monophosphatase YktC.

Corynebacterium glutamicum is a Gram-positive actinobacterium that has become a model organism in industrial biotechnology due its use in large-scale amino acid production (Eggeling and Bott, 2005; Eggeling and Bott, 2015; Wendisch et al., 2016). Meanwhile, *C. glutamicum* strains for the synthesis of many other products besides amino acids have been developed (Becker and Wittmann, 2012; Freudl, 2017; Heider and Wendisch, 2015; Wieschalka et al., 2013) *C. glutamicum* can utilize a broad variety of carbon sources, including *myo*-inositol (Krings et al., 2006). When cultivated with *myo*-inositol, more than 20 genes showed increased expression, the majority of which was located in two clusters on the genome. Cluster I contains genes that are essential for growth on *myo*-inositol, whereas the genes of cluster II are dispensable for *myo*-inositol degradation (Krings et al., 2006). Cluster II encodes amongst others several putative oxidoreductases that had the ability to compensate loss of the IolG function encoded in cluster I and thus must contain at least one gene encoding an additional *myo*-inositol dehydrogenase (Krings et al., 2006). Two secondary transporters for *myo*-inositol were identified in *C. glutamicum* and characterized, called IolT1 (Cg0223) and IolT2 (Cg3387). IolT1 and IolT2 share 55% sequence identity and comparable kinetic constants with K_m values

of 0.22 and 0.45 mM and V_{max} values of 1.22 and 2.90 nmol min^{-1} (mg cells)$^{-1}$, respectively (Krings et al., 2006). The expression of the genes of cluster I and of *iolT1* is repressed by the GntR-type transcriptional regulator IolR in the absence of *myo*-inositol (Klaffl et al., 2013).

In contrast to *B. subtilis*, *C. glutamicum* is not only able to degrade *myo*-inositol, but also has the intrinsic capability to synthesize *myo*-inositol from glucose 6-phosphate. In the order *Corynebacteriales*, which includes the genus *Mycobacterium*, *myo*-inositol is required for the synthesis of mycothiol, the analog of glutathione in this bacterial group (Newton et al., 2008), and of phosphatidylinositol, an abundant phospholipid in the cytoplasmic membrane and the precursor of more complex lipids of the cell envelope such as phosphatidylinositol mannosides, lipomannan, and lipoarabinomannan (Morita et al., 2011). *Myo*-inositol is formed by first converting glucose 6-phosphate to L-*myo*-inositol 1-phosphate with *myo*-inositol phosphate synthase (Ino1, Cg3323) followed by dephosphorylation with *myo*-inositol phosphate monophosphatase (ImpA, Cg2298). Expression of the *ino1* gene is activated by the LacI-type transcriptional regulator IpsA, which itself is inactivated by binding of *myo*-inositol, causing dissocation of IpsA from its DNA targets (Baumgart et al., 2013).

Based on the available knowledge on *myo*-inositol metabolism and a preliminary bioinformatic analysis of the multiple inositol dehydrogenase genes encoded in the genome, we considered *C. glutamicum* as an interesting alternative host for *scyllo*-inositol production. In this study, we show the natural ability of *C. glutamicum* to produce and consume *scyllo*-inositol when cultivated in the presence of *myo*-inositol and identified the responsible enzymes. By metabolic engineering, we obtained strains enabling efficient conversion of *myo*-inositol into *scyllo*-inositol. Finally, we designed strains that were able to produce high titers of *scyllo*-inositol from the cheap carbon source sucrose.

2. Materials and Methods

2.1 Bacterial strains, plasmids and growth conditions

All bacterial strains and plasmids used in this work are listed in Table 1. All cloning steps were performed with *Escherichia coli* DH5α as host. *E. coli* strains were cultivated at 37 °C on LB agar plates or in lysogeny broth (LB) (Bertani, 1951) with 50 µg/mL kanamycin. *C. glutamicum* was cultivated in baffled shake flasks at 130 rpm at 30 °C using either brain heart infusion (BHI) medium (Difco Laboratories, Detroit, USA) or defined CGXII medium (Keilhauer et al., 1993) with 0.03 g/L protocatechuic acid, which were supplemented with either 20 g/L glucose, 20 g/L *myo*-inositol, 20 g/L each of glucose and *myo*-inositol, or 20 g/L sucrose as carbon and energy sources. Where appropriate, 25 µg/mL kanamycin was added to the medium. Bacterial growth was followed by measuring the optical density at 600 nm (OD_{600}). To start cultivation, 10 mL BHI medium in a 100 mL baffled shake flask was inoculated with a single colony from an agar plate and incubated overnight at 30 °C and 130 rpm. The main culture was inoculated to an initial OD_{600} of 0.5. Main cultures in BHI medium were inoculated directly from overnight precultures. For inoculation of main cultures in CGXII medium, cells of the preculture were harvested and washed twice in CGXII medium. Target gene expression was induced via addition of isopropyl-β-D-thiogalactoside (IPTG) as indicated in the results sections.

2.2 Recombinant DNA work and construction of deletion mutants

All plasmids and oligonucleotides used in this study are listed in Tables 1 and 2, respectively. Routine methods such as PCR and DNA restriction were performed using established protocols (Green and Sambrook, 2012). Transformation of *E. coli* was performed according to an established protocol (Hanahan, 1983). Transformation of *C. glutamicum* was performed by electroporation (van der Rest et al., 1999). Plasmids were constructed via Gibson assembly (Gibson et al., 2009). DNA sequencing and oligonucleotide synthesis were performed by Eurofins Genomics (Ebersberg, Germany). The deletion mutant *C. glutamicum*

MB001(DE3)Δ*iol1* was constructed via double homologous recombination as described previously using pK19mobsacBΔ*iol1* (Niebisch and Bott, 2001). The double deletion mutant *C. glutamicum* MB001(DE3)Δ*iol1*Δ*iol2* was constructed in the same way using plasmid pK19mobsacBΔ*iol2*. The chromosomal deletions were confirmed via colony-PCR using oligonucleotides annealing outside of the deleted region. For both deletions, 25% of the tested clones after the second recombination event contained the desired deletion, whereas 75% showed the wild-type situation, showing that none of deleted genes was essential for growth in the media used.

For the construction of the expression plasmids pIolGW and pSI, all corresponding genes were first cloned separately into the plasmid pMKEx2 downstream of the *C. glutamicum* consensus ribosome binding site (RBS). All genes were then again amplified together with the RBS using the designated primer pairs and cloned as synthetic operons in pMKEx2 via Gibson assembly. For the expression plasmids, pMKEx2-*oxiC*, pMKEx2-*oxiD*, pMKEx2-*oxiE*, pMKEx2-*idhA3* and pMKEx2-cg3390 the corresponding genes were amplified by PCR from chromosomal DNA and then cloned via Gibson assembly into pMKE2 downstream of the *C. glutamicum* consensus RBS.

2.3 Inositol analysis by HPLC

1 mL culture was centrifuged at 17,000 *g* for 20 min, the supernatant was filtered (0.2 µm syringe filter, Whatman™, GE Healthcare, Freiburg, Germany) and frozen at -20 °C until further analysis. Thawed samples were diluted with deionized water and applied for HPLC analysis. A 10 µL sample was measured using an Agilent LC-1100 system (Agilent, Santa Clara, CA, USA) equipped with a Carbo-Ca Guard Catridge (Phenomenex, Aschaffenburg, Germany) and a Rezex RCM-Monosaccharide 300 x 7.8 mm column (Phenomenex, Aschaffenburg, Germany). Separation was performed at 80 °C with water as eluent at a flow rate of 0.6 mL/min. Sugar and sugar alcohols were detected with a refraction index detector operated at 35 °C. The retention times were 11 min for glucose, 8.5 min for sucrose, 14.5 min for *myo*-inositol, and 12.1 min for *scyllo*-inositol.

2.4 Protein overproduction, SDS-PAGE and inositol dehydrogenase activity assays

C. glutamicum MB001(DE3)Δ*iol1*Δ*iol2* was transformed with pMKEx2-based plasmids for expression of various inositol dehydrogenases and cultivated in BHI medium supplemented with 20 g/L glucose. Overexpression of the target genes was induced after 3 h with 100 µM IPTG and cells were harvested after 24 h of cultivation via centrifugation (30 min at 5,100 g and 4°C). Cell pellets were washed and resuspended in 4 mL lysis buffer (100 mM Tris-HCl pH 7.5, 1 mM $MgSO_4$) per g cell wet weight and disrupted using 0.1 mm zirconia/silica beads (BioSpec Products Inc., Bartlesville, USA) in a MM2 mixer mill (Retsch GmbH, Haan, Germany). Whole cell lysates were cleared by centrifugation at 13,000 *g* and 4 °C for 20 min. Equal amounts of protein (10 µg per lane) were analyzed by SDS-PAGE according to standard procedures (Green and Sambrook, 2012). Proteins were visualized by Coomassie Brilliant Blue staining. The inositol dehydrogenase activity assay was performed as described previously (Bakkes et al., 2020) with final concentrations of 25 mM *myo*-inositol or *scyllo*-inositol as substrates and 1 mM NAD^+ or 1 mM $NADP^+$ as coenzymes.

3. Results and Discussion

3.1 Bioinformatic analysis of the C. glutamicum protein repertoire for the presence of inositol dehydrogenases

The conversion of *myo*-inositol to *scyllo*-inositol involves *myo*-inositol dehydrogenase and *scyllo*-inositol dehydrogenase. Analysis of the proteins encoded by the *C. glutamicum* genome with the *B. subtilis myo*-inositol dehydrogenase $IolG_{Bs}$ as query resulted in the identification of four proteins with an identity >26%, which have been annotated as IolG (Cg0204), IdhA3 (Cg2313), OxiE (Cg3392), and OxiD (Cg3391) (Table 3, Fig. 1). IolG was recently purified and shown to have a specific NAD^+-dependent *myo*-inositol dehydrogenase activity of 27 μmol min^{-1} (mg protein)$^{-1}$ (Bakkes et al., 2020). In addition, IolG also catalyzes the oxidation of D-xylose to D-xylonate (Tenhaef et al., 2018). Expression of *iolG*, *oxiE*, and *oxiD* was strongly upregulated in *myo*-inositol-grown cells (Krings et al., 2006), whereas expression of *idhA3* was not altered, suggesting a different regulation. As the *iolG* inactivation mutant WT::p*iolG'* was still able to grow with *myo*-inositol, but not a WTΔ*oxiII*::p*iolG'* double mutant lacking also *oxiC*, *oxiD*, and *oxiE* (Krings et al., 2006), OxiD and/or OxiE most likely have *myo*-inositol dehydrogenase activity. With the *scyllo*-inositol dehydrogenase IolW of *B. subtilis* as query two proteins were identified in *C. glutamicum*, which are OxiA, renamed IolW now (Cg0207), and OxiC (Cg3389). With the *scyllo*-inositol dehydrogenase IolX of *B. subtilis* as query three related proteins were found in *C. glutamicum*, which are IdhA3 (Cg2313), OxiD (Cg3391), and OxiE (Cg3392) (Table 3).

3.2 Scyllo-inositol formation from myo-inositol by C. glutamicum

The results of the bioinformatic analysis suggested that *C. glutamicum* might possess the capabilities to synthesize and to degrade *scyllo*-inositol. Therefore, we performed a shake flask experiment in which *C. glutamicum* MB001(DE3) was cultivated in CGXII minimal medium

with either 20 g/L glucose, or 20 g/L *myo*-inositol, or 20 g/L of each glucose and *myo*-inositol as carbon and energy source. Growth was similar for all three conditions (Fig. 2A, D, and G), except that the cultures with both carbon sources reached a higher final OD_{600}. When cultivated with *myo*-inositol, *C. glutamicum* secreted up to 1 g/L *scyllo*-inositol within the first 10 h, which was depleted again after 24 hours (Fig. 2F). In contrast, no *scyllo*-inositol was formed during growth with glucose (Fig. 2C). When cultivated with a mixture of glucose and *myo*-inositol, a maximal titer of 2 g/L *scyllo*-inositol was formed after 24 h, which disappeared within the next 24 h (Fig. 2I). These results show that *C. glutamicum* naturally produces *scyllo*-inositol when cultivated in the presence of *myo*-inositol.

3.3. Construction and characterization of C. glutamicum chassis strains for scyllo-inositol production from myo-inositol

For an efficient biotechnological production of *scyllo*-inositol from *myo*-inositol by *C. glutamicum*, a strain which is unable to catabolize *myo*-inositol is mandatory. Previous studies showed that genes of cluster I (cg0196-cg0223) are required for inositol catabolism, whereas the genes of cluster II (cg3385-cg3395) are not (Krings et al., 2006). Based on this information, we constructed two deletion mutants. *C. glutamicum* MB001(DE3)Δ*iol1* lacks 16 genes (cg0196-cg0212) present in cluster I and *C. glutamicum* MB001(DE3)Δ*iol1*Δ*iol2* additionally lacks four genes (cg3389-3392) located in cluster II (Fig. 1). Growth, *myo*-inositol consumption, and *scyllo*-inositol production of these strains were analyzed during cultivation in shake flasks with CGXII medium containing either 20 g/L glucose, 20 g/L *myo*-inositol, or 20 g/L each of glucose and *myo*-inositol (Fig. 2). Both deletion mutants grew slightly faster ($\mu = 0.44\ h^{-1}$) than the parental strain ($\mu = 0.37\ h^{-1}$) when cultivated on glucose (Fig. 2A), which correlated with a faster glucose consumption (Fig. 2B). This difference is presumably caused by the strongly increased expression of *iolT1* (>70-fold increased mRNA level) caused by the deletion of *iolR* (Fig. 1) encoding the transcriptional regulator IolR (Cg0196), which represses

iolT1 in the absence of *myo*-inositol (Klaffl et al., 2013). IolT1 is a secondary transporter with a relaxed substrate specifity, which does not only transport *myo*-inositol, but also glucose (Ikeda et al., 2011; Lindner et al., 2011) and xylose (Brüsseler et al., 2018). IolT1 provides an additional pathway for glucose uptake besides the glucose-specific phosphotransferase system PtsG. The overall glucose uptake capacity is thus increased.

When cultivated with *myo*-inositol as sole carbon and energy source, the *C. glutamicum* chassis strains MB001(DE3)Δ*iol1* and MB001(DE3)Δ*iol1*Δ*iol2* showed no growth (Fig. 2D), as all seven genes proposed to be involved in the catabolism of *myo*-inositol to dihydroxyacetone phosphate, acetyl-CoA and CO_2 (*iolG, iolE, iolD, iolB, iolC, iolJ*, and *iolA*) were removed by the Δ*iol1* deletion (Fig. 1). Accordingly, *myo*-inositol was not consumed and no *scyllo*-inositol was formed (Fig. 2F). When cultivated in medium with 20 g/L glucose and 20 g/L *myo*-inositol, the two chassis strains showed impaired growth ($\mu = 0.18\ h^{-1}$) and slowed glucose consumption compared to the parental strain MB001(DE3) ($\mu = 0.41\ h^{-1}$) (Fig. 2G and H). One reason for this difference is probably the reduced uptake of glucose via IolT1 in the presence of *myo*-inositol. The K_m value for *myo*-inositol of IolT1 was determined as 0.22 mM (Krings et al., 2006), whereas for glucose a K_s value of 2.3 mM was reported (Lindner et al., 2011). Therefore, glucose uptake via IolT1 is expected to be outcompeted by *myo*-inositol. However, this difference does not explain the strongly reduced growth rate, as glucose can still be taken up by PtsG. We assume that accumulation of *myo*-inositol or products formed from *myo*-inositol within the cells of strains MB001(DE3)Δ*iol1* and MB001(DE3)Δ*iol1*Δ*iol2* cause inhibitory effects on metabolism, which are responsible for slowed growth and glucose consumption.

Interestingly, strain MB001(DE3)Δ*iol1* consumed ~5 g/L *myo*-inositol and formed ~1 g/L *scyllo*-inositol within 24 h, which was not degraded later on (Fig. 2I). Concomitantly, the medium became brown. In contrast, the mutant MB001(DE3)Δ*iol1*Δ*iol2* did not consume *myo*-inositol or produce *scyllo*-inositol (Fig. 2I) and the medium did not become brown. These

results suggest that one or several of the three dehydrogenases (OxiC, OxiD, OxiE) encoded in the Δ*iol2* region are responsible for the conversion of *myo*-inositol to *scyllo*-inositol in strain MB001(DE3)Δ*iol1*. Only about 20% of the *myo*-inositol consumed by strain MB001(DE3)Δ*iol1* was converted to *scyllo*-inositol and therefore also other products must have been formed. Since strain MB001(DE3)Δ*iol1*Δ*iol2* did not consume appreciable amounts of *myo*-inositol, its utilization for the synthesis of mycothiol, phosphatidylinositol and derived lipids cannot explain the missing 80% of *myo*-inositol. As shown below, the conversion of 2-keto-*myo*-inositol to unknown products causing brown coloration is presumably responsible for the difference between *myo*-inositol consumption and *scyllo*-inositol production by strain MB001(DE3)Δ*iol1*.

3.4 Production of scyllo-inositol from myo-inositol in defined medium

In the next step for efficient *scyllo*-inositol production from *myo*-inositol, we used the *myo*-inositol dehydrogenase IolG, whose activity has been confirmed (Bakkes et al., 2020), and the putative *scyllo*-inositol dehydrogenase IolW, since it showed the highest identity to $IolW_{Bs}$ of *B. subtilis* (Tanaka et al., 2013). The other putative inositol dehydrogenases were not included, since they showed similar identities to several reference proteins (Table 3), among them IolX, which is an NAD^+-dependent *scyllo*-inositol dehydrogenase responsible for *scyllo*-inositol oxidation (Morinaga et al., 2010). We cloned the genes *iolG* (cg0204) and *iolW* (cg0207) of *C. glutamicum* as a synthetic operon into the plasmid pMKEx2 under control of the T7 promoter to enable strong, IPTG-inducible expression in the MB001(DE3) background (Kortmann et al., 2015). The resulting plasmid pIolGW and the control plasmid pMKEx2-*eyfp* were transferred into MB001(DE3)Δ*iol1* and MB001(DE3)Δ*iol1*Δ*iol2* and the recombinant strains were cultivated in CGXII medium with 20 g/L each of glucose and *myo*-inositol. The strains with pIolGW showed a slightly diminished growth rate compared to the strains with pMKEx2-*eyfp*

(Fig. 3A and B). Expression of *iolG* and *iolW* was induced at the start of the cultivation with 100 µM IPTG.

Whereas the two strains with pMKEx2-*eyfp* displayed a comparable behavior with respect to *myo*-inositol consumption as the plasmid-free strains (Fig. 2), the strains with pIolGW showed remarkable differences (Fig. 3C-F). Strain MB001(DE3)Δ*iol1* with pIolGW completely consumed *myo*-inositol within 48 h and formed a maximal titer of 2.5 g/L *scyllo*-inositol after 24 h, which subsequently decreased to 1.2 g/L after 72 h (Fig. 3C and E). Strain MB001(DE3)Δ*iol1*Δ*iol2* with pIolGW consumed only 11 g/L *myo*-inositol within 72 h, but formed a titer of 4.4 g/L *scyllo*-inositol within 24 h, which remained constant until the end of the cultivation (Fig. 3D and F). Moreover, this strain also accumulated 2.7 g/L 2-keto-*myo*-inositol after 72 h. This intermediate was not detectable in the Δ*iol1* strain. When looking at the balance, the fate of 18.8 g/L *myo*-inositol consumed by strain MB001(DE3)Δ*iol1* remains unknown, whereas for strain MB001(DE3)Δ*iol1*Δ*iol2* it is 3.9 g/L. This suggested that in MB001(DE3)Δ*iol1* further products are formed, e.g. by the enzymes encoded in the Δ*iol2* region and elsewhere in the genome, as also for MB001(DE3)Δ*iol1*Δ*iol2* the balance was not closed.

As shown in Fig. 3G, the two strains with pIolGW also differed with respect to the color of the cultures. The supernatant of strain MB001(DE3)Δ*iol1* became brown within 24 h and the intensity increased further at 48 h. We speculate that the brown coloration is caused by Maillard reaction products that are formed by reactions of reducing sugars and free amino groups (Ajandouz et al., 2001; Ledl and Schleicher, 1990; Stadler et al., 2002). As this color was not observed in the supernatant of strain MB001(DE3)Δ*iol1*Δ*iol2*, enzymes encoded in the Δ*iol2* region are probably responsible for the formation of the brown color. The supernatant of strain MB001(DE3)Δ*iol1*Δ*iol2* showed only a slight change of color within 24 h and became yellow-orange within 48 h. This color is due to the formation of 2-keto-*myo*-inositol, as it was also

observed when this compound (obtained by Sigma Aldrich) was dissolved in CGXII medium, while dissolved *scyllo*-inositol caused no color change (data not shown).

3.5 Analysis of proteins encoded by the Δ*iol2* region and by *idhA3*

To investigate if one or more of the residual dehydrogenases are responsible for the loss of *myo*- and *scyllo*-inositol observed in the experiments shown in Fig. 3, we individually overproduced the putative inositol dehydrogenases OxiC, OxiD, OxiE, and IdhA3 in *C. glutamicum* MB001(DE3)Δ*iol1*Δ*iol2* using the pMKEx2 expression vector (Fig. S1). Subsequently we determined the specific dehydrogenase activity for *myo*-inositol and *scyllo*-inositol using cell-free extracts and NAD^+ or $NADP^+$ as coenzyme (Table 4). Extracts containing OxiC and IdhA3 showed no activity for either tested inositol. In contrast, extracts containing OxiD and OxiE catalyzed the NAD^+-dependent oxidation of *myo*-inositol with specific activities of 22.59 ± 0.03 μmol min^{-1} mg^{-1} and 2.68 ± 0.04 μmol min^{-1} mg^{-1}. Therefore, the consumption of *myo*-inositol by strain MB001(DE3)Δ*iol1* observed in Fig. 2I and the residual growth observed for a *iolG* mutant in a previous study (Krings et al., 2006) can be explained by the *myo*-inositol dehydrogenase activity of OxiD and OxiE.

Interestingly, OxiE showed an even higher specific activity for *scyllo*-inositol with NAD^+ as favored cofactor (11.06 ± 0.18 μmol min^{-1} mg^{-1}), revealing a function similar to the catabolic *scyllo*-inositol dehydrogenase IolX of *B. subtilis* (Morinaga et al., 2010). This suggests that OxiE mainly functions in oxidizing *scyllo*-inositol to 2-keto-*myo*-inositol and thus counteracts *scyllo*-inositol formation by IolW. Therefore, it can be assumed that OxiE contributes to *scyllo*-inositol consumption observed in the *C. glutamicum* strains possessing the *iol2* cluster (Fig. 2F and I and Fig. 3C).

As 2-keto-*myo*-inositol was only detected in the MB001(DE3)Δ*iol1*Δ*iol2* strain, but not in the Δ*iol1* strain although the latter consumed much more *myo*-inositol (Fig. 3), we assumed that

2-keto-*myo*-inositol is converted to other products in the Δ*iol1* strain by enzymes encoded in the Δ*iol2* region, resulting in the proposed Maillard products and the dark brown coloration. Since we showed that OxiD and OxiE function as *myo*- and/or *scyllo*-inositol dehydrogenases (Table 4), we considered them unlikely to be responsible for a different kind of 2-keto-*myo*-inositol conversion and brown coloration. Rather, we focused on the putative sugar phosphate isomerase Cg3390 and OxiC as potential causes for the conversion of 2-keto-*myo*-inositol to further, unknown products. To test their role in the formation of the brown color, we cloned *oxiC* and cg3390 individually and in combination with *iolG* into pMKEx2, introduced the resulting plasmids in *C. glutamicum* MB001(DE3)Δ*iol1*Δ*iol2*, and cultivated the strains at 30°C in CGXII medium with 20 g/L glucose and 20 g/L *myo*-inositol. Gene expression was induced via addition of 100 µM IPTG at the beginning of the cultivation. After 72 h, we examined the color and determined the concentrations of *myo*-inositol and 2-keto-*myo*-inositol (Fig. 4). Cultures in which cg3390, *oxiC*, or as control *eyfp* were overexpressed showed no color change and no *myo*-inositol consumption. Strains expressing either *iolG* or *iolG-oxiC* consumed part of the *myo*-inositol and formed approximately 4.0 g/L of 2-keto-*myo*-inositol, associated with yellow coloration, but not *scyllo*-inositol. Most interestingly, the strain expressing *iolG* together with cg3390 showed dark brown coloration (Fig. 4A) and no residual *myo*-inositol or 2-keto-*myo*-inositol was present after 72 h (Fig. 4B). This result proves that Cg3390 is responsible for the conversion of 2-keto-*myo*-inositol to unknown products causing brown coloration.

3.6 Production of scyllo-inositol from myo-inositol in rich medium

As the *scyllo*-inositol yield from *myo*-inositol in CGXII medium was maximally 0.4 g/g, we tested whether the use of rich BHI medium, which is often used for cultivation of *C. glutamicum*, could increase the yield. Previous studies with *B. subtilis* reported a positive effect of increased peptone concentrations on *scyllo*-inositol formation from *myo*-inositol (Tanaka et al., 2017). We analyzed *scyllo*-inositol formation by *C. glutamicum* MB001(DE3)Δ*iol1* and

MB001(DE3)Δ*iol1*Δ*iol2* containing either pIolGW or pMKEx-*eyfp* during growth in BHI medium containing 20 g/L each of glucose and *myo*-inositol. Expression of the target genes was induced at the start of the cultivation with 100 µM IPTG. Again, the strains with pIolGW showed a slightly diminished growth rate compared to the strains with pMKEx2-*eyfp* (Fig. 5A and B). Strain MB001(DE3)Δ*iol1* with pIolGW produced ~15 g/L *scyllo*-inositol from 20 g/L *myo*-inositol after 72 h, with ~1 g/L *myo*-inositol remaining in the medium. 4 g/L *myo*-inositol was converted into unknown products (Fig. 5C, E). Increasingly brown coloration of medium supernatants was observed during the cultivation, but much less intense than in CGXII medium (Fig. 5G). Based on the results described in the previous section, conversion of 2-keto-*myo*-inositol by the Cg3390 enzyme is probably responsible for synthesis of the unknown products and the brown color. Strain MB001(DE3)Δ*iol1*Δ*iol2* with pIolGW formed 18 g/L *scyllo*-inositol from 18 g/L consumed *myo*-inositol and the residual 2 g/L *myo*-inositol remained unmetabolized. Thus, the entire *myo*-inositol consumed was converted into *scyllo*-inositol (Fig. 5D, F). In these cultures, the color of the medium remained almost unchanged (Fig. 5G).

In conclusion, the deletion of the *iol2* region proved to be important for the biotechnological production of *scyllo*-inositol with *C. glutamicum*, since the activities of at least two enzymes encoded in this region counteract *scyllo*-inositol formation. OxiE oxidizes *scyllo*-inositol formed in an NADPH-dependent reaction by IolW back to 2-keto-*myo*-inositol using NAD^+ as coenzyme. The putative isomerase Cg3390 converts 2-keto-*myo*-inositol to a yet unknown product that is probably further converted to Maillard products. Besides the Δ*iol2* deletion, the use of BHI instead of CGXII medium enabled a much better conversion of *myo*-inositol into *scyllo*-inositol and strongly reduced the formation of compounds assumed to be Maillard products. Furthermore, no accumulation of 2-keto-*myo*-inositol was observed for strain MB001(DE3)Δ*iol1*Δ*iol2* with pIolGW in BHI medium in contrast to CGXII medium. This suggests that the reduction of 2-keto-*myo*-inositol to *scyllo*-inositol is a bottleneck in CGXII medium. A possible explanation for the difference is a lowered NADPH demand for biomass

synthesis in BHI medium compared to CGXII medium. BHI medium contains amino acids and peptides, which are taken up by the cells and used for the synthesis of proteins, which make up about 50% of the cell dry weight. In CGXII medium, all amino acids need to be synthesized from glucose and ammonia, which is associated with a high NADPH demand. For example, synthesis of one mol lysine from oxaloacetate requires four moles NADPH. Therefore, during cultivation in CGXII medium a large fraction of the NADPH formed in the oxidative PPP and a few other reactions is used for biomass synthesis and not available for reduction of 2-keto-*myo*-inositol to *scyllo*-inositol.

3.7 Production of scyllo-inositol from glucose and sucrose

The experimental setup described above allowed efficient production of *scyllo*-inositol from *myo*-inositol, but as this compound is still quite expensive, we aimed to replace it by cheaper carbon sources such as glucose or sucrose. As described in the introduction, *C. glutamicum* has the natural ability to synthesize *myo*-inositol from glucose 6-phosphate in a two-step pathway involving *myo*-inositol 1-phosphate synthase (Ino1) and *myo*-inositol 1-phosphatase (ImpA). We therefore constructed the pMKEx2-based expression plasmid pSI, which contains a synthetic operon comprising the genes *ino1*, *impA*, *iolG*, and *iolW* under the control of the T7 promoter. The *C. glutamicum* strains MB001(DE3)Δ*iol1* and MB001(DE3)Δ*iol1*Δ*iol2* were transformed with pSI or the control plasmid pMKEx2-*eyfp* and cultivated in BHI medium with 20 g/L glucose or 20 g/L sucrose.

When cultivated in the presence of glucose or sucrose, the strains containing the control plasmid pMKEx2-*eyfp* consumed glucose or sucrose completely within 24 h or 32 h, respectively, and did not form *scyllo*-inositol (Fig. 6). The strains containing pSI showed decelerated growth (after ~4 h) on glucose, but not on sucrose (Fig. 6A, D), whereas consumption was slowed down for both, glucose and sucrose (Fig. 6B, E). The reason for the negative effect of the presence of the pSI plasmid is not clear yet. One explanation could be an

unspecific dephosphorylation of phosphorylated metabolites besides *myo*-inositol 1-phosphate by the overproduced phosphatase ImpA, causing a deceleration of central metabolism. Examples for such unspecific activities have been reported e.g. for the 3′-phosphoadenosine-5′-phosphatase CysQ of *Mycobacterium tuberculosis*, which besides the natural substrate also dephosphorylates *myo*-inositol 1-phosphate and fructose 1,6-bisphosphate (Hatzios et al., 2008).

Production of *scyllo*-inositol from glucose started after 12 h and reached titers of 0.8 g/L for MB001(DE3)Δ*iol1* pSI and 1.8 g/L for MB001(DE3)Δ*iol1*Δ*iol2* pSI after 72 h (Fig. 6C). A slight drop of the *scyllo*-inositol concentration was observed between 48 h and 72 h for the Δ*iol1* strain, whereas it still increased in that period for the Δ*iol1*Δ*iol2* strain. This effect and difference in titers are most likely due to the activities of of OxiE and Cg3390 (see above). Production of *scyllo*-inositol from sucrose started after ~8 h and reached titers of 3.9 g/L for MB001(DE3)Δ*iol1* pSI and 4.4 g/L for MB001(DE3)Δ*iol1*Δ*iol2* pSI after 72 h (Fig. 6F). The majority of *scyllo*-inositol was formed when the cultures were in the stationary growth phase. No 2-keto-*myo*-inositol formation was observed in supernatant samples and no color change occurred for both strains cultivated on either glucose or sucrose.

The increase in *scyllo*-inositol production with sucrose as substrate instead of glucose is presumably linked to the differences in the metabolism of these sugars (Blombach and Seibold, 2010), shown in Fig. 7. Glucose is taken up by PtsG forming glucose 6-phosphate, or by IolT1 followed by phosphorylation via Glk (Cg2399) or PpgK (Cg2091) to glucose 6-phosphate. Sucrose is taken up by the sucrose-specific PTS (PtsS), forming sucrose 6-phosphate, which is then hydrolyzed by ScrB into fructose and glucose 6-phosphate. Fructose is exported by an unknown carrier and then reimported by the fructose-specific PTS (PtsF) to form fructose 1-phosphate, which is phosphorylated by fructose 1-phosphate kinase (PfkB) to fructose 1,6-bisphosphate. In a study on the carbon flux of sucrose in a lysine-producing strain of *C. glutamicum*, the glucose part of sucrose was completely channeled into the PPP, whereas the

fructose part was predominantly metabolized in glycolysis (Wittmann et al., 2004). When cells are grown on glucose alone, a large fraction of glucose 6-phosphate is channeled into glycolysis, which varies between 73% and 26% depending on the NADPH demand of the cells (Marx et al., 1997). We speculate that there is a higher concentration and availability of glucose 6-phosphate in sucrose-grown cells, which is responsible for the increased *scyllo*-inositol production. The first enzyme for channeling glucose 6-phosphate into the inositol pathway is *myo*-inositol 1-phosphate synthase (Ino1). For Ino1 of *C. glutamicum* a K_m value of 12 mM for glucose 6-phosphate and a k_{cat} of 2.24 min^{-1} has been reported (Chen et al., 2019). In contrast, the competing glucose 6-phosphate dehydrogenase (G6PDH) of *C. glutamicum*, which catalyzes the irreversible oxidation to 6-phosphogluconolactone, has a K_m value of 169 µM for glucose 6-phosphate and a specific activity of 160 U/mg (Moritz et al., 2000). In view of these differences, an increased glucose 6-phosphate concentration might be a major reason for increased *scyllo*-inositol production from sucrose by enabling higher Ino1 activity.

4. Conclusions

The results of this study identify *C. glutamicum* as a promising host for the production of *scyllo*-inositol, a potential drug against Alzheimer's disease. Using strains defective in *myo*-inositol and *scyllo*-inositol metabolism that overexpressed the genes *iolG* and *iolW* we could achieve a complete conversion of *myo*-inositol to *scyllo*-inositol in rich medium. Additional overexpression of the genes *ino1* and *impA* enabled *scyllo*-inositol production from glucose with a yield (1.8 g/20 g glucose) comparable to the one reported for *B. subtilis* (Michon et al., 2020). However, sucrose turned out to be a better substrate than glucose, as 4.4 g *scyllo*-inositol were formed from 20 g sucrose. Our next studies aim at a further increase of the production of *scyllo*-inositol and other *myo*-inositol-derived compounds from cheap carbon sources by metabolic engineering approaches aiming at a redirection of carbon flux towards *myo*-inositol,

examples of which were reported e.g. for glucarate production in *E. coli* (Brockman and Prather, 2015; Doong et al., 2018).

Author contributions

Paul Ramp: Conceptualization, Methodology, Investigation, Writing – Initial Draft, Visualization. Alexander Lehnert: Methodology, Investigation. Susana Matamouros: Methodology, Supervision. Astrid Wirtz: Methodology, Investigation. Meike Baumgart: Methodology, Writing - Original Draft, Supervision. Michael Bott: Conceptualization, Writing – Review and Editing, Supervision, Funding acquisition.

Declaration of competing interest

The authors declare no conflict of interests.

Acknowledgments

This project was financially supported by the CLIB-Competence Center Biotechnology (CKB) funded by the European Regional Development Fund ERDF [grant number 34.EFRE-0300097] and by the German Federal Ministry of Education and Research (BMBF) [grant number 031B0918A], as part of the project "BiookonomieREVIER".

References

Ajandouz, E. H., Tchiakpe, L. S., Dalle Ore, F., Benajiba, A., Puigserver, A., 2001. Effects of pH on caramelization and Maillard reaction kinetics in fructose-lysine model systems. J. Food Sci. 66**,** 926-931.

Bakkes, P. J., Ramp, P., Bida, A., Dohmen-Olma, D., Bott, M., Freudl, R., 2020. Improved pEKEx2-derived expression vectors for tightly controlled production of recombinant proteins in *Corynebacterium glutamicum*. Plasmid 112**,** 102540.

Baumgart, M., Luder, K., Grover, S., Gätgens, C., Besra, G. S., Frunzke, J., 2013. IpsA, a novel LacI-type regulator, is required for inositol-derived lipid formation in Corynebacteria and Mycobacteria. BMC Biol. 11**,** 122.

Becker, J., Wittmann, C., 2012. Bio-based production of chemicals, materials and fuels–*Corynebacterium glutamicum* as versatile cell factory. Curr. Opin. Biotechnol. 23**,** 631-640.

Bertani, G., 1951. Studies on lysogenesis. The mode of phage liberation by lysogenic *Escherichia coli*. J. Bacteriol. 62**,** 293-300.

Blombach, B., Seibold, G. M., 2010. Carbohydrate metabolism in *Corynebacterium glutamicum* and applications for the metabolic engineering of L-lysine production strains. Appl. Microbiol. Biotechnol. 86**,** 1313-1322.

Brockman, I. M., Prather, K. L. J., 2015. Dynamic knockdown of *E. coli* central metabolism for redirecting fluxes of primary metabolites. Metab. Eng. 28**,** 104-113.

Brüsseler, C., Radek, A., Tenhaef, N., Krumbach, K., Noack, S., Marienhagen, J., 2018. The myo-inositol/proton symporter IolT1 contributes to D-xylose uptake in *Corynebacterium glutamicum*. Bioresour. Technol. 249**,** 953-961.

Candy, D. J., 1967. Occurrence and metabolism of scylloinositol in the locust. Biochem. J. 103**,** 666-71.

Chen, C., Chen, K., Su, T., Zhang, B., Li, G., Pan, J., Si, M., 2019. *Myo*-inositol-1-phosphate synthase (Ino-1) functions as a protection mechanism in *Corynebacterium glutamicum* under oxidative stress. MicrobiologyOpen. 8**,** e00721.

Doong, S. J., Gupta, A., Prather, K. L. J., 2018. Layered dynamic regulation for improving metabolic pathway productivity in *Escherichia coli*. Proc. Natl. Acad. Sci. USA 115**,** 2964-2969.

Eggeling, L., Bott, M., 2005. Handbook of *Corynebacterium glutamicum*. CRC Press, Boca Raton.

Eggeling, L., Bott, M., 2015. A giant market and a powerful metabolism: L-lysine provided by *Corynebacterium glutamicum*. Appl. Microbiol. Biotechnol. 99**,** 3387-3394.

Fenili, D., Brown, M., Rappaport, R., McLaurin, J., 2007. Properties of *scyllo*-inositol as a therapeutic treatment of AD-like pathology. J. Mol. Med. 85**,** 603-611.

Freudl, R., 2017. Beyond amino acids: use of the *Corynebacterium glutamicum* cell factory for the secretion of heterologous proteins. J. Biotechnol. 258**,** 101-109.

Gibson, D. G., Young, L., Chuang, R. Y., Venter, J. C., Hutchison, C. A., Smith, H. O., 2009. Enzymatic assembly of DNA molecules up to several hundred kilobases. Nat. Meth. . 6**,** 343-345.

Green, M. R., Sambrook, J., 2012. Molecular Cloning. A Laboratory Manual. Cold Spring Harbor Laboratory Press, Cold Spring Harbor, New York.

Hanahan, D., 1983. Studies on transformation of *Escherichia coli* with plasmids. J. Mol. Biol. 166**,** 557-580.

Hatzios, S. K., Iavarone, A. T., Bertozzi, C. R., 2008. Rv2131c from M*ycobacterium tuberculosis* is a CysQ 3'-phosphoadenosine-5'-phosphatase. Biochemistry. 47**,** 5823-5831.

Heider, S. A., Wendisch, V. F., 2015. Engineering microbial cell factories: Metabolic engineering of *Corynebacterium glutamicum* with a focus on non-natural products. Biotechnol. J. 10**,** 1170-1184.

Horner, W. H., Thaker, I. H., 1968. Metabolism of *scyllo*-inositol in *Streptomyces griseus*. Biochim. Biophys. Acta. 165**,** 306-308.

Ikeda, M., Mizuno, Y., Awane, S., Hayashi, M., Mitsuhashi, S., Takeno, S., 2011. Identification and application of a different glucose uptake system that functions as an alternative to the phosphotransferase system in *Corynebacterium glutamicum*. Appl. Microbiol. Biotechnol. 90**,** 1443-1451.

Keilhauer, C., Eggeling, L., Sahm, H., 1993. Isoleucine synthesis in *Corynebacterium glutamicum*: molecular analysis of the *ilvB-ilvN-ilvC* operon. J. Bacteriol. 175**,** 5595-5603.

Klaffl, S., Brocker, M., Kalinowski, J., Eikmanns, B. J., Bott, M., 2013. Complex regulation of the phosphoenolpyruvate carboxykinase gene *pck* and characterization of its GntR-type regulator IolR as a repressor of *myo*-inositol utilization genes in *Corynebacterium glutamicum*. J. Bacteriol. 195**,** 4283-4296.

Kortmann, M., Kuhl, V., Klaffl, S., Bott, M., 2015. A chromosomally encoded T7 RNA polymerase-dependent gene expression system for *Corynebacterium glutamicum*: construction and comparative evaluation at the single-cell level. Microb. Biotechnol. 8**,** 253-265.

Krings, E., Krumbach, K., Bathe, B., Kelle, R., Wendisch, V. F., Sahm, H., Eggeling, L., 2006. Characterization of *myo*-inositol utilization by *Corynebacterium glutamicum*: the stimulon, identification of transporters, and influence on L-lysine formation. J. Bacteriol. 188**,** 8054-8061.

Ledl, F., Schleicher, E., 1990. New aspects of the Maillard reaction in foods and in the human body. Angew. Chem. Int. Ed. 29**,** 565-594.

Li, Y., Han, P., Wang, J., Shi, T., You, C., 2021. Production of *myo*-inositol: Recent advances and prospective. Biotechnol. Appl. Biochem., 1-11

Lindner, S. N., Seibold, G. M., Henrich, A., Krämer, R., Wendisch, V. F., 2011. Phosphotransferase system-independent glucose utilization in *Corynebacterium glutamicum* by inositol permeases and glucokinases. Appl. Environm. Microbiol. 77**,** 3571-3581.

Marx, A., Striegel, K., de Graaf, A. A., Sahm, H., Eggeling, L., 1997. Response of the central metabolism of *Corynebacterium glutamicum* to different flux burdens. Biotechnol. Bioeng. 56**,** 168-180.

McLaurin, J., Kierstead, M. E., Brown, M. E., Hawkes, C. A., Lambermon, M. H. L., Phinney, A. L., Darabie, A. A., Cousins, J. E., French, J. E., Lan, M. F., Chen, F. S., Wong, S. S. N., Mount, H. T. J., Fraser, P. E., Westaway, D., St George-Hyslop, P., 2006. Cyclohexanehexol inhibitors of Aβ aggregation prevent and reverse Alzheimer phenotype in a mouse model. Nat. Med. 12**,** 801-808.

Michon, C., Kang, C. M., Karpenko, S., Tanaka, K., Ishikawa, S., Yoshida, K. I., 2020. A bacterial cell factory converting glucose into *scyllo*-inositol, a therapeutic agent for Alzheimer's disease. Comm. Biol. 3**,** 93.

Morinaga, T., Ashida, H., Yoshida, K., 2010. Identification of two *scyllo*-inositol dehydrogenases in *Bacillus subtilis*. Microbiology. 156**,** 1538-1546.

Morita, Y. S., Fukuda, T., Sena, C. B., Yamaryo-Botte, Y., McConville, M. J., Kinoshita, T., 2011. Inositol lipid metabolism in mycobacteria: biosynthesis and regulatory mechanisms. Biochim. Biophys. Acta. 1810**,** 630-641.

Moritz, B., Striegel, K., De Graaf, A. A., Sahm, H., 2000. Kinetic properties of the glucose-6-phosphate and 6-phosphogluconate dehydrogenases from *Corynebacterium glutamicum* and their application for predicting pentose phosphate pathway flux in vivo. Eur. J. Biochem. 267**,** 3442-3452.

Newton, G. L., Buchmeier, N., Fahey, R. C., 2008. Biosynthesis and functions of mycothiol, the unique protective thiol of Actinobacteria. Microbiol. Mol. Biol. Rev. 72**,** 471-494.

Niebisch, A., Bott, M., 2001. Molecular analysis of the cytochrome bc_1-aa_3 branch of the *Corynebacterium glutamicum* respiratory chain containing an unusual diheme cytochrome c_1. Arch. Microbiol. 175**,** 282-294.

Salloway, S., Sperling, R., Keren, R., Porsteinsson, A. P., van Dyck, C. H., Tariot, P. N., Gilman, S., Arnold, D., Abushakra, S., Hernandez, C., Crans, G., Liang, E., Quinn, G., Bairu, M., Pastrak, A., Cedarbaum, J. M., ELND005-AD201 Investigators, 2011. A phase 2 randomized trial of ELND005, *scyllo*-inositol, in mild to moderate Alzheimer disease. Neurology 77**,** 1253-1262.

Sarmah, M. P., Shashldhar, M. S., 2003. Sulfonate protecting groups. Improved synthesis of *scyllo*-inositol and its orthoformate from *myo*-inositol. Carbohyd. Res. . 338**,** 999-1001.

Schäfer, A., Tauch, A., Jäger, W., Kalinowski, J., Thierbach, G., Pühler, A., 1994. Small mobilizable multi-purpose cloning vectors derived from the *Escherichia coli* plasmids pK18 and pK19: selection of defined deletions in the chromosome of *Corynebacterium glutamicum*. Gene 145**,** 69-73.

Stadler, R. H., Blank, I., Varga, N., Robert, F., Hau, J., Guy, P. A., Robert, M. C., Riediker, S., 2002. Acrylamide from Maillard reaction products. Nature. 419**,** 449-450.

Tanaka, K., Natsume, A., Ishikawa, S., Takenaka, S., Yoshida, K., 2017. A new-generation of *Bacillus subtilis* cell factory for further elevated *scyllo*-inositol production. Microb Cell Fact. 16.

Tanaka, K., Tajima, S., Takenaka, S., Yoshida, K.-i. J. M. c. f., 2013. An improved *Bacillus subtilis* cell factory for producing *scyllo*-inositol, a promising therapeutic agent for Alzheimer's disease. Microb. Cell Fact. 12**,** 124.

Tenhaef, N., Brüsseler, C., Radek, A., Hilmes, R., Unrean, P., Marienhagen, J., Noack, S., 2018. Production of D-xylonic acid using a non-recombinant *Corynebacterium glutamicum* strain. Bioresour. Technol. 268**,** 332-339.

Townsend, M., Cleary, J. P., Mehta, T., Hofmeister, J., Lesne, S., O'Hare, E., Walsh, D. M., Selkoe, D. J., 2006. Orally available compound prevents deficits in memory caused by the Alzheimer amyloid-beta oligomers. Ann. Neurol. . 60**,** 668-676.

van der Rest, M. E., Lange, C., Molenaar, D., 1999. A heat shock following electroporation induces highly efficient transformation of *Corynebacterium glutamicum* with xenogeneic plasmid DNA. Appl. Microbiol. Biotechnol. 52**,** 541-545.

Wenda, S., Illner, S., Mell, A., Kragl, U., 2011. Industrial biotechnology—the future of green chemistry? Green Chem. 13**,** 3007-3047.

Wendisch, V. F., Jorge, J. M., Pérez-García, F., Sgobba, E., 2016. Updates on industrial production of amino acids using *Corynebacterium glutamicum*. World J. Microbiol. Biotechnol. 32**,** 105.

Wieschalka, S., Blombach, B., Bott, M., Eikmanns, B., 2013. Bio-based production of organic acids with *Corynebacterium glutamicum*. Microb. Biotechnol. 6**,** 87-102.

Wittmann, C., Kiefer, P., Zelder, O., 2004. Metabolic fluxes in *Corynebacterium glutamicum* during lysine production with sucrose as carbon source. Appl. Environ. Microbiol. 70**,** 7277-7287.

Yamaoka, M., Osawa, S., Morinaga, T., Takenaka, S., Yoshida, K., 2011. A cell factory of *Bacillus subtilis* engineered for the simple bioconversion of *myo*-inositol to *scyllo*-inositol, a potential therapeutic agent for Alzheimer's disease. Microb Cell Fact. 10.

Yoshida, K. I., Aoyama, D., Ishio, I., Shibayama, T., Fujita, Y., 1997. Organization and transcription of the *myo*-inositol operon, *iol*, of *Bacillus subtilis*. J. Bacteriol. 179**,** 4591-4598.

Yoshida, K. I., Yamaguchi, M., Ikeda, H., Omae, K., Tsurusaki, K. I., Fujita, Y., 2004. The fifth gene of the *iol* operon of *Bacillus subtilis*, *iolE*, encodes 2-keto-*myo*-inositol dehydratase. Microbiology. 150**,** 571-580.

Yoshida, K. I., Yamaguchi, M., Morinaga, T., Kinehara, M., Ikeuchi, M., Ashida, H., Fujita, Y., 2008. *myo*-Inositol catabolism in *Bacillus subtilis*. J. Biol. Chem. 283**,** 10415-10424.

Table 1. Bacterial strains and plasmids used in this study.

Strain or plasmid	Relevant characteristics	Source or reference
E. coli		
DH5α	F^- Φ80*dlac*Δ(*lacZ*)M15 Δ(*lacZYA-argF*) U169 *endA1 recA1 hsdR17* (r_K^- , m_K^+) *deoR thi-1 phoA supE44* λ^- *gyrA96 relA1*; strain used for cloning procedures	(Hanahan, 1983)
C. glutamicum		
MB001(DE3)	prophage-free derivate of ATCC 13032 with chromosomal expression of T7 RNA polymerase gene under control of P_{lac}UV5 (IPTG-inducible)	(Kortmann et al., 2015)
MB001(DE3)Δ*iol1*	MB001(DE3) derivative with deletion of the genes cg0196-cg0212	This work
MB001(DE3)Δ*iol1* Δ*iol2*	MB001(DE3) Δ*iol1* derivative with deletion of the genes cg3389-cg3392	This work
Plasmids		
pK19*mobsacB*	Kan^R; plasmid for allelic exchange in *C. glutamicum*; (pK18 *ori*$V_{E.c.}$, *sacB*, *lacZ*α)	(Schäfer et al., 1994)
pK19*mobsacB*Δ*iol1*	Kan^R; pK19*mobsacB* derivative containing two 1-kb PCR products which cover the upstream flanking region of *iolR* (cg0196) and the downstream flanking region of *iolE2* (cg0212)	This work
pK19*mobsacB*Δ*iol2*	Kan^R; pK19*mobsacB* derivative containing two 1-kb PCR products which cover the upstream flanking region of *oxiC* (cg3388) and the downstream flanking region of *oxiE* (cg3393)	This work
pMKEx2	Kan^R; *E. coli-C. glutamicum* shuttle vector (*lacI*, P_{T7}, lacO1, pHM1519 ori $_{Cg}$; pACYC177 ori $_{Ec}$) for expression of target genes under control of the T7 promoter	(Kortmann et al., 2015)
pMKEx2-*eyfp*	Kan^R; pMKEx2 derivative containing the *eyfp* gene under control of P_{T7}	(Kortmann et al., 2015)
pIolGW	Kan^R; pMKEx2 derivative containing the *C. glutamicum* genes *iolG* (cg0204) and *iolW* (cg0207) as a synthetic operon under control of the T7 promoter	This work
pSI	Kan^R; pMKEx2 derivative containing the *C. glutamicum* genes *ino1* (cg3323), *impA* (cg2298), *iolG* (cg0204) and iolW (cg0207) as synthetic operon under control of the T7 promoter	This work
pMKEx2-*iolG*	Kan^R; pMKEx2 derivative containing the *C. glutamicum* gene *iolG* (cg0204) under control of P_{T7}	This work

pMKEx2-*iolW*	Kan^R; pMKEx2 derivative containing the *C. glutamicum* gene *iolW* (cg0207) under control of P_{T7}	This work
pMKEx2-*oxiC*	Kan^R; pMKEx2 derivative containing the *C. glutamicum* gene *oxiC* (cg3389) under control of P_{T7}	This work
pMKEx2-*oxiD*	Kan^R; pMKEx2 derivative containing the *C. glutamicum* gene *oxiD* (cg3391) under control of P_{T7}	This work
pMKEx2-*oxiE*	Kan^R; pMKEx2 derivative containing the *C. glutamicum* gene *oxiE* (cg3392) under control of P_{T7}	This work
pMKEx2-*idhA3*	Kan^R; pMKEx2 derivative containing the *C. glutamicum* gene *idhA3* (cg2313) under control of P_{T7}	This work
pMKEx2-cg3390	Kan^R; pMKEx2 derivative containing the *C. glutamicum* gene cg3390 under control of P_{T7}	This work
pMKEx2-*iolG-oxiC*	Kan^R; pMKEx2 derivative containing the *C. glutamicum* genes *iolG* (cg0204) and *oxiC* (cg3389) as a synthetic operon under control of the T7 promoter	This work
pMKEx2-*iolG*-cg3390	Kan^R; pMKEx2 derivative containing the *C. glutamicum* genes *iolG* (cg0204) and cg3390 as a synthetic operon under control of the T7 promoter	This work

Table 2. Oligonucleotides used in this study.

Oligonucleotide name	Oligonucleotide sequence (5'→ 3')
Construction pK19mobsacBΔ*iol1*	
P001_Δiol1_FW1	GAGGATCCCCGGGTACCGAGCTCGTTCCGCCAACTCAACC
P002_Δiol1_RV1	TGAAACCACTCTGGTGGCCAGGTAAG
P003_Δiol1_FW2	CTTACCTGGCCACCAGAGTGGTTTCAGAAGAGTCCCTGGTTTC
P004_Δiol1_RV2	CGTTGTAAAACGACGGCCAGTGAATTTCCTTGGTCACCAGATC
P005_Seq_pK19_FW	AGCGGATAACAATTTCACACAGGA
P006_Seq_pK19_RV	CGCCAGGGTTTTCCCAGTCAC
Construction pK19mobsacBΔ*iol2*	
P007_ΔoxiC-E_FW1	GAGGATCCCCGGGTACCGAGCTCGGGAACCCAATTCACCTTCG
P008_ΔoxiC-E_RV1	GCCTAGCAGGCCAACAAC
P009_ΔoxiC-E_FW2	AAATTGTTGTTGGCCTGCTAGGCTGCGCTGGTTCCATCTGC
P010_ΔoxiC-E_RV2	CGTTGTAAAACGACGGCCAGTGAATTGGACCAACCAGAAACTTC
P005_Seq_pK19_FW	AGCGGATAACAATTTCACACAGGA
P006_Seq_pK19_RV	CGCCAGGGTTTTCCCAGTCAC
Construction of individual pMKEx2 plasmids	
P011_iolW_pMKEx2_FW	ACTTTAAGAAGGAGATATACCATGACTATTCGAATCGGACTCG
P012_iolW_pMKEx2_RV	TGGCACCAGAGCGAGCTCTGCGGCCTTAGCTCAACTCAATGGTGCG
P013_iolG_pMKEx2_FW	ACTTTAAGAAGGAGATATACCATGAGCAAGAGCCTTCGC
P014_iolG_pMKEx2_RV	TGGCACCAGAGCGAGCTCTGCGGCCTTAAGCGTAGAAATCTGGGCG
P015_impA_pMKEx2_FW	CTTTAAGAAGGAGATATACCATGGATGCTCGTGGGATGTTG
P016_impA_pMKEx2_RV	GGTGGCTCCAGCTTGCCATGTTACTTGTACTCCTCATTTAACG
P041_oxiC_pMKEx2_FW	CTTTAAGAAGGAGATATACCATGAGTGATCAAAAAATTG
P042_oxiC_pMKEx2_RV	CCAGAGCGAGCTCTGCGGCCTTAGATGTTTACGGAAATGCC
P043_cg3390_pMKEx2_FW	CTTTAAGAAGGAGATATACCATGAAACCACAACTTATTG
P044_cg3390_pMKEx2_RV	GAGCGAGCTCTGCGGCCTCAGTTAGTGGAGGGGGC
P045_oxiD_pMKEx2_FW	CTTTAAGAAGGAGATATACCATGACTCTTCGTATCGCC
P046_oxiD_pMKEx2_RV	CCAGAGCGAGCTCTGCGGCCCTAAACGTTGGCAGGGTTGAG
P047_oxiE_pMKEx2_FW	CTTTAAGAAGGAGATATACCATGAAAAACATCACCATCGG
P048_oxiE_pMKEx2_RV	CCAGAGCGAGCTCTGCGGCCTTAAGCAGATGGAACCAGCG
P049_idhA3_pMKEx2_FW	CTTTAAGAAGGAGATATACCATGTCAGTCAAACTTGCCCTC
P050_idhA3_pMKEx2_RV	CCAGAGCGAGCTCTGCGGCCTTAAACCTCGATGCTTTCAG
P017_Seq_pMKEx2_FW	AGGAGATGGCGCCCAACAG
P018_Seq_pMKEx2_RV	ACTTTGCGCAGCTCAGG
Construction of pIolG-W	
P013_iolG_pMKEx2_FW	ACTTTAAGAAGGAGATATACCATGAGCAAGAGCCTTCGC
P019_iolG_iolG-IolW_RV	TGTCGCTCAGAGACCTGAGGTTAAGCGTAGAAATCTGGGCGAG
P020_iolW_iolG-IolW_FW	CCTCAGGTCTCTGAGCGACAGAAGGAGATATACCATG
P012_iolW_pMKEx2_RV	CCAGAGCGAGCTCTGCGGCCTTAGCTCAACTCAATGGTG
P021_Seq_iolG1	GTGTTGGTGAGAGCTAC
P022_Seq_iolW1	AAAGCAGCCGTTGCAG
P023_Seq_iolW2	CGGCTCCTACGTATC
P017_Seq_pMKEx2_FW	AGGAGATGGCGCCCAACAG
P018_Seq_pMKEx2_RV	ACTTTGCGCAGCTCAGG

Construction of pSI

P024_ino1_ino1-impA-iolG-iolW_FW	CTTTAAGAAGGAGATATACCATGAGCACGTCCACCATCAG
P025_ino1_ino1-impA-iolG-iolW_RV	GCAGGTGCACAATGATACGATTACGCCTCGATGATGAATG
P026_impA_ino1-impA-iolG-iolW_FW	TCGTATCATTGTGCACCTGCGAAGGAGATATACCATG
P027_impA_ino1-impA-iolG-iolW_RV	ACATCGTTGAGTGGTCACCGTTACTTGTACTCCTCATTTAAC
P028_iolG_ino1-impA-iolG-iolW_FW	CGGTGACCACTCAACGATGTGAAGGAGATATACCATG
P029_iolG_ino1-impA-iolG-iolW_RV	TGTCGCTCAGAGACCTGAGGTTAAGCGTAGAAATCTGGGCGAG
P030_iolW_ino1-impA-iolG-iolW_FW	CCTCAGGTCTCTGAGCGACAGAAGGAGATATACCATG
P012_iolW_pMKEx2_RV	TGGCACCAGAGCGAGCTCTGCGGCCTTAGCTCAACTCAATGGTGCG
P021_Seq_iolG1	GTGTTGGTGAGAGCTAC
P022_Seq_oxiA1	AAAGCAGCCGTTGCAG
P023_Seq_oxiA2	CGGCTCCTACGTATC
P017_Seq_pMKex2_FW	AGGAGATGGCGCCCAACAG
P018_Seq_pMKex2_RV	ACTTTGCGCAGCTCAGG
P031_ino1_pSI_Seq	TTGGTGTCCTACCTCC
P032_impA_pSI_Seq1	AGCAGCTTCCAGACGATG
P033_impA_pSI_Seq2	AGCATGCGTATCGTTTAG

Construction of pMKEx2-*iolG-oxiC*

P013_iolG_pMKEx2_FW	ACTTTAAGAAGGAGATATACCATGAGCAAGAGCCTTCGC
P051_iolG_iolG-oxiC_RV	CTTTCAGAAGTGGGTTTCTCCTTAAGCGTAGAAATC
P052_iolG-oxiC_pMKEx2-FW	GAGAAACCCACTTCTGAAAGGAGAATTCCCATGAGTGATC
P042_oxiC_pMKEx2_RV	CCAGAGCGAGCTCTGCGGCCTTAGATGTTTACGGAAATGCC

Construction of pMKEx2-*iolG*-cg3390

P013_iolG_pMKEx2_FW	ACTTTAAGAAGGAGATATACCATGAGCAAGAGCCTTCGC
P019_iolG_iolG-IolW_RV	TGTCGCTCAGAGACCTGAGGTTAAGCGTAGAAATCTGGGCGAG
P053_cg3390_iolG-cg3390_FW	CTCAGGTCTCTGAGCGACAAGAGGAGCACTCCATG
P044_cg3390_pMKEx2_RV	GAGCGAGCTCTGCGGCCTCAGTTAGTGGAGGGGGC

Recombination analysis Δ*iol1*

P034_Col_deliol_FW	GGGATTTCGTTGCCATG
P035_Col_deliolR-E2_RV	GGTTGCGGCAATCTTCC
P036_Seq_deliol1	CTGGACCAAACCAGGTG

Recombination analysis Δ*iol2*

P037_Col_deloxiC-E_FW	ACACCATCCGGGACAC
P038_Col_deloxiC-E_RV1	CGTTCAAGACGTCATC
P039_Col_deloxiC-E_RV2	ACTGCAATGCTGGCCTG
P040_Seq_delOxiC-E_1	CGTGGAACTGATCCTG

Table 3. *C. glutamicum* proteins showing homology to the *B. subtilis* inositol dehydrogenases IolG, IolW, and IolX. The analysis was performed with BLAST function of the ERGO Bioinformatics suite (Igenbio Inc., Chicago, USA).

Query protein of *B. subtilis*	Homologs in *C. glutamicum* (with cg number)	Alignment length (amino acids)	E-value	% Identity
IolG (344 aa)	IolG (Cg0204)	335	2e-78	39.10
	IdhA3 (Cg2313)	352	3e-33	29.55
	OxiD (Cg3391)	332	3e-28	26.81
	OxiE (Cg3392)	309	8e-21	27.18
IolW (358 aa)	IolW (OxiA) (Cg0207)	353	1e-45	30.88
	OxiC (Cg3389)	309	5e-12	24.60
IolX (342 aa)	IdhA3 (Cg2313)	334	8e-56	36.83
	OxiD (Cg3391)	332	1e-50	32.83
	OxiE (Cg3392)	304	4e-45	31.58

Table 4. Specific *myo*-inositol and *scyllo*-inositol dehydrogenase activities in cell-free extracts of *C. glutamicum* MB001(DE3)Δ*iol1*Δ*iol2* overproducing six known or putative inositol dehydrogenases. Dehydrogenase activity was determined in a spectrophotometric assay by measuring the absorbance increase at 340 nm in an assay mixture containing cell-free extract, 1 mM of cofactor (either NAD^+ or $NADP^+$) and either 25 mM *myo*-inositol or 25 mM *scyllo*-inositol. Mean values and standard deviations of three technical replicates are shown.

Protein overproduced	Coenzyme	Specific activity for *myo*-inositol (µmol min^{-1} mg^{-1})	Specific activity for *scyllo*-inositol (µmol min^{-1} mg^{-1})
eYFP	NAD^+	n. d.	n. d.
(negative control)	$NADP^+$	n. d.	n. d.
OxiC	NAD^+	n. d.	n. d.
	$NADP^+$	n. d.	n. d.
OxiD	NAD^+	22.59 ± 0.03	n. d.
	$NADP^+$	1.11 ± 0.12	n. d.
OxiE	NAD^+	2.68 ± 0.04	11.06 ± 0.18
	$NADP^+$	n. d.	0.32 ± 0.05
IdhA3	NAD^+	n. d.	n. d.
	$NADP^+$	n. d.	n. d.

n.d. : not detected

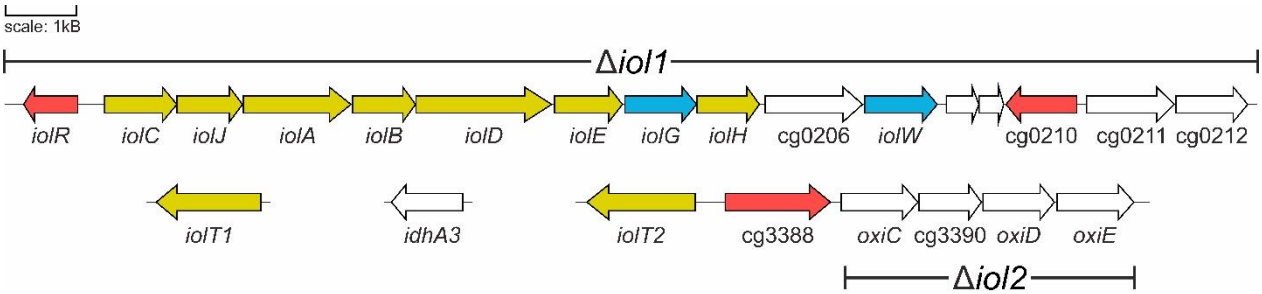

Fig. 1. Genes related to inositol catabolism in *C. glutamicum*. The genomic regions deleted in this work are indicated as Δ*iol1* and Δ*iol2*. Genes shown in red encode transcriptional regulators, genes in yellow have a known or predicted function, and genes in white have putative or unknown functions. The genes *iolG* and *iolW* used in this study for the production of *scyllo*-inositol are highlighted in blue.

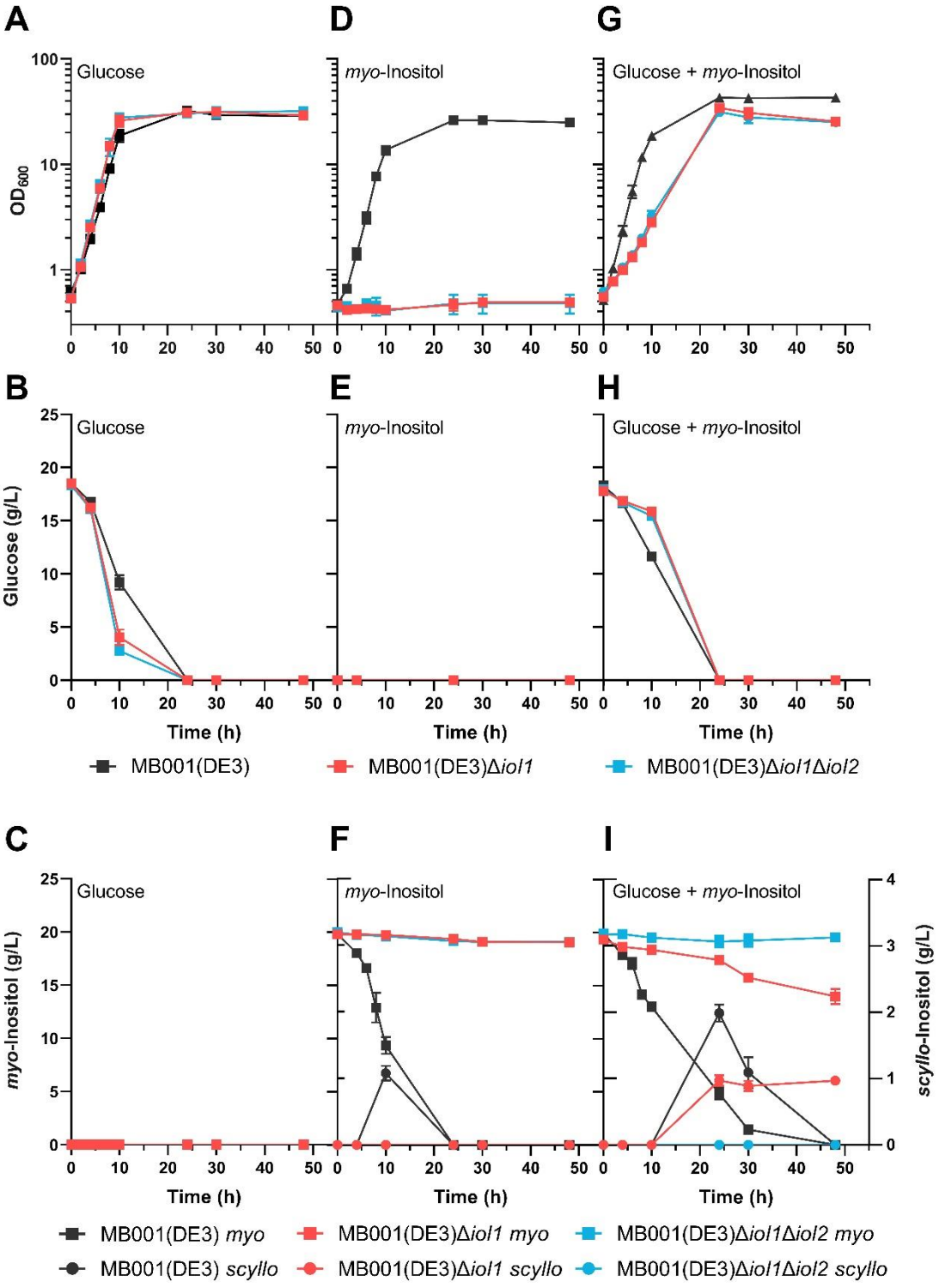

Fig. 2. Growth (OD_{600}), *myo*-inositol consumption (*myo*) and *scyllo*-inositol formation (*scyllo*), and glucose consumption of the indicated *C. glutamicum* strains in CGXII medium containing either 20 g/L glucose (panels A, B, C), or 20 g/L *myo*-inositol (panels D, E, F), or 20 g/L each

of glucose and *myo*-inositol (panels G, H, I). Mean values of biological triplicates and standard deviation are shown.

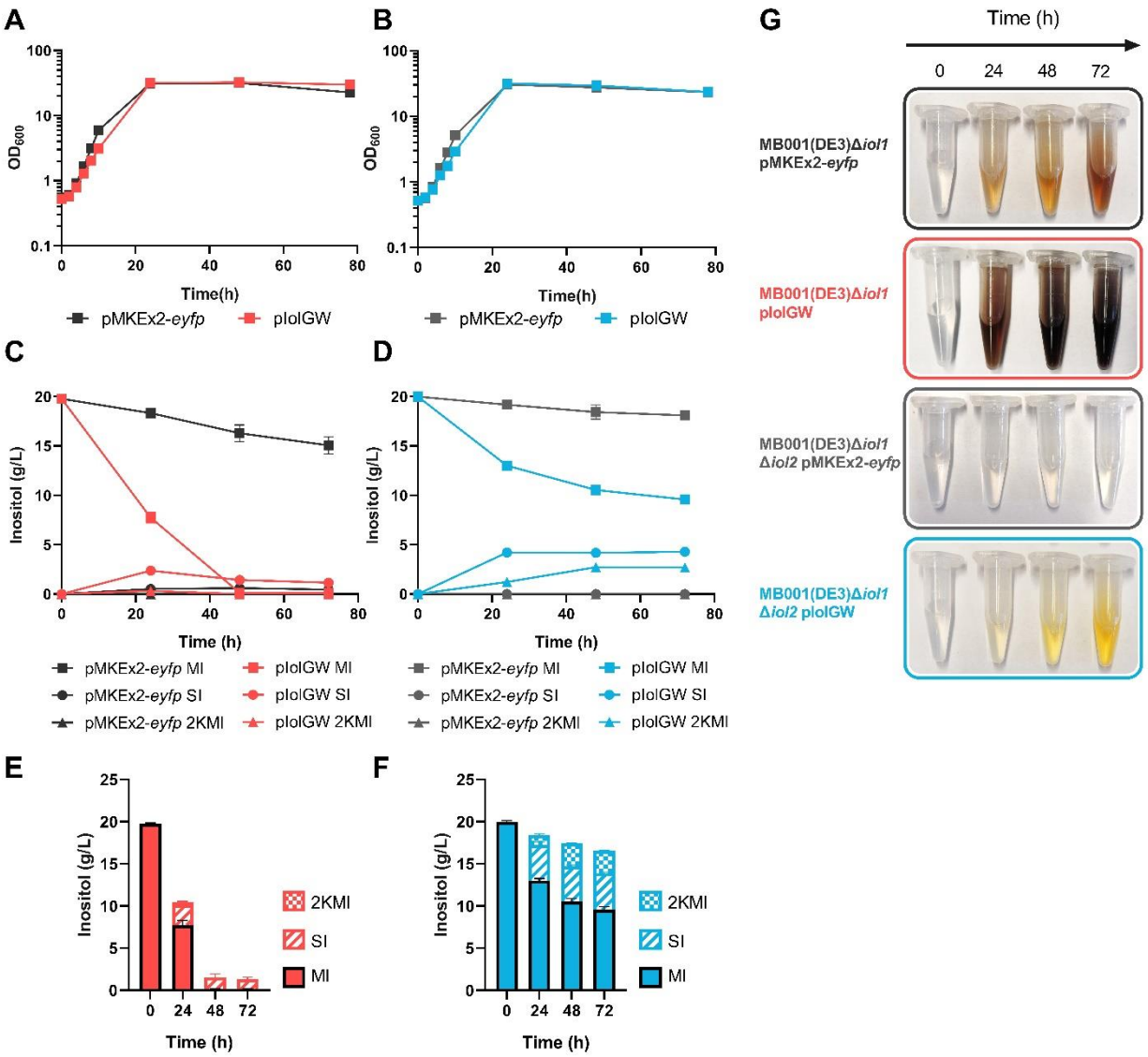

Fig. 3. Production of *scyllo*-inositol from *myo*-inositol in CGXII medium with 20 g/L each of glucose and *myo*-inositol. Panels A and B show growth, panels C and D the kinetics of *myo*-inositol (MI) consumption and formation of *scyllo*-inositol (SI) and 2-keto-*myo*-inositol (2KMI) of the *C. glutamicum* strains MB001(DE3)Δ*iol1* (panels A and C) and MB001(DE3)Δ*iol1*Δ*iol2* (panels B and D) carrying either pMKEx2-*eyfp* or pIolGW. Panels E and F show the sum of the different inositol concentrations detected at the indicated time points for strain MB001(DE3)Δ*iol1* with pIolGW (E) and MB001(DE3)Δ*iol1*Δ*iol2* with pIolGW (F). Panel G shows photographs of supernatant samples of the indicated strain at the indicated time

points during cultivation. For A-F, mean values and standard deviations of three biological replicates are shown.

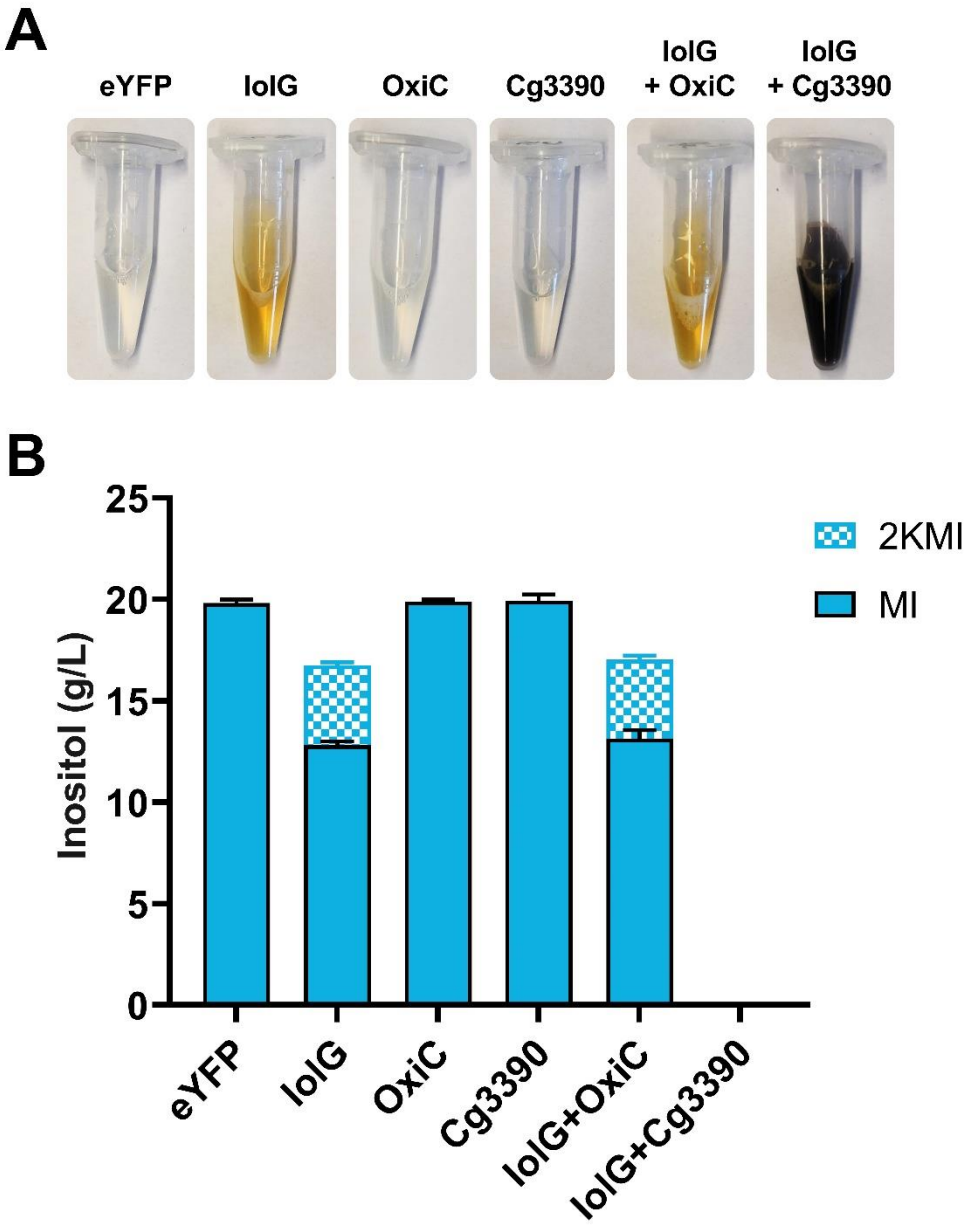

Fig. 4. Influence of plasmid-based overproduction of the indicated proteins in *C. glutamicum* MB001(DE3)Δ*iol1*Δ*iol2* on the color of the medium (A) and the concentrations of *myo*-inositol (MI) and 2-keto-*myo*-inositol (2KMI) (B) after 72 h of growth at 30°C in CGXII medium with 20 g/L glucose and 20 g/L *myo*-inositol.

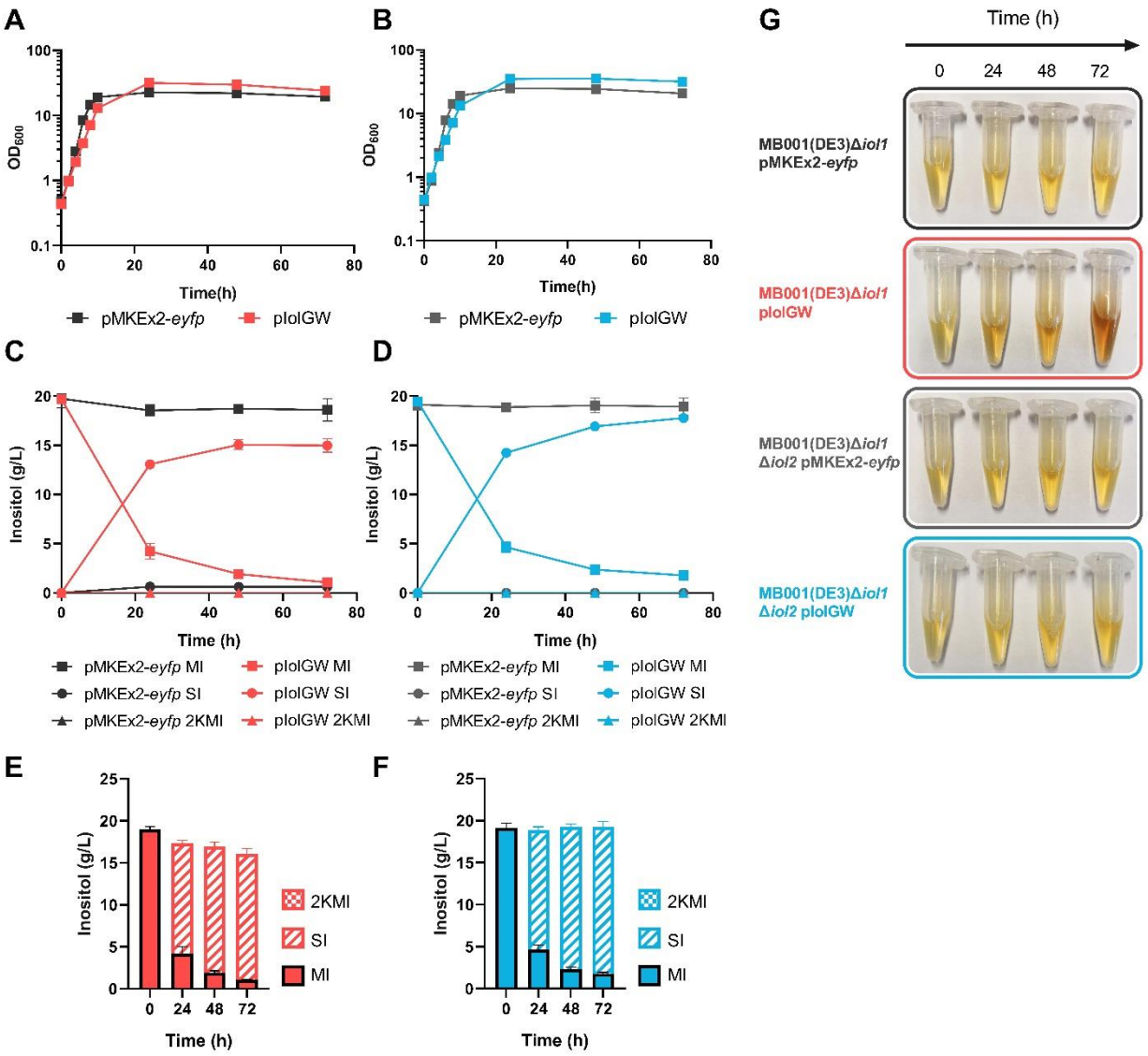

Fig. 5. Production of *scyllo*-inositol from *myo*-inositol in BHI medium with 20 g/L each of glucose and *myo*-inositol. Panels A and B show growth, panels C and D show the kinetics of *myo*-inositol (MI) consumption and formation of *scyllo*-inositol (SI) and 2-keto-*myo*-inositol (2KMI) of the *C. glutamicum* strains MB001(DE3)Δ*iol1* (panels A and C) and MB001(DE3)Δ*iol1*Δ*iol2* (panels B and D) carrying either pMKEx2-*eyfp* or pIolGW. Panels E and F show the sum of the different inositol concentrations detected at the indicated time points for strain MB001(DE3)Δ*iol1* with pIolGW (B) and MB001(DE3)Δ*iol1*Δ*iol2* with pIolGW (D). Panel G shows photographs of supernatant samples of the indicated strain at the indicated time

points during cultivation. For A-F, mean values and standard deviations of three biological replicates are shown.

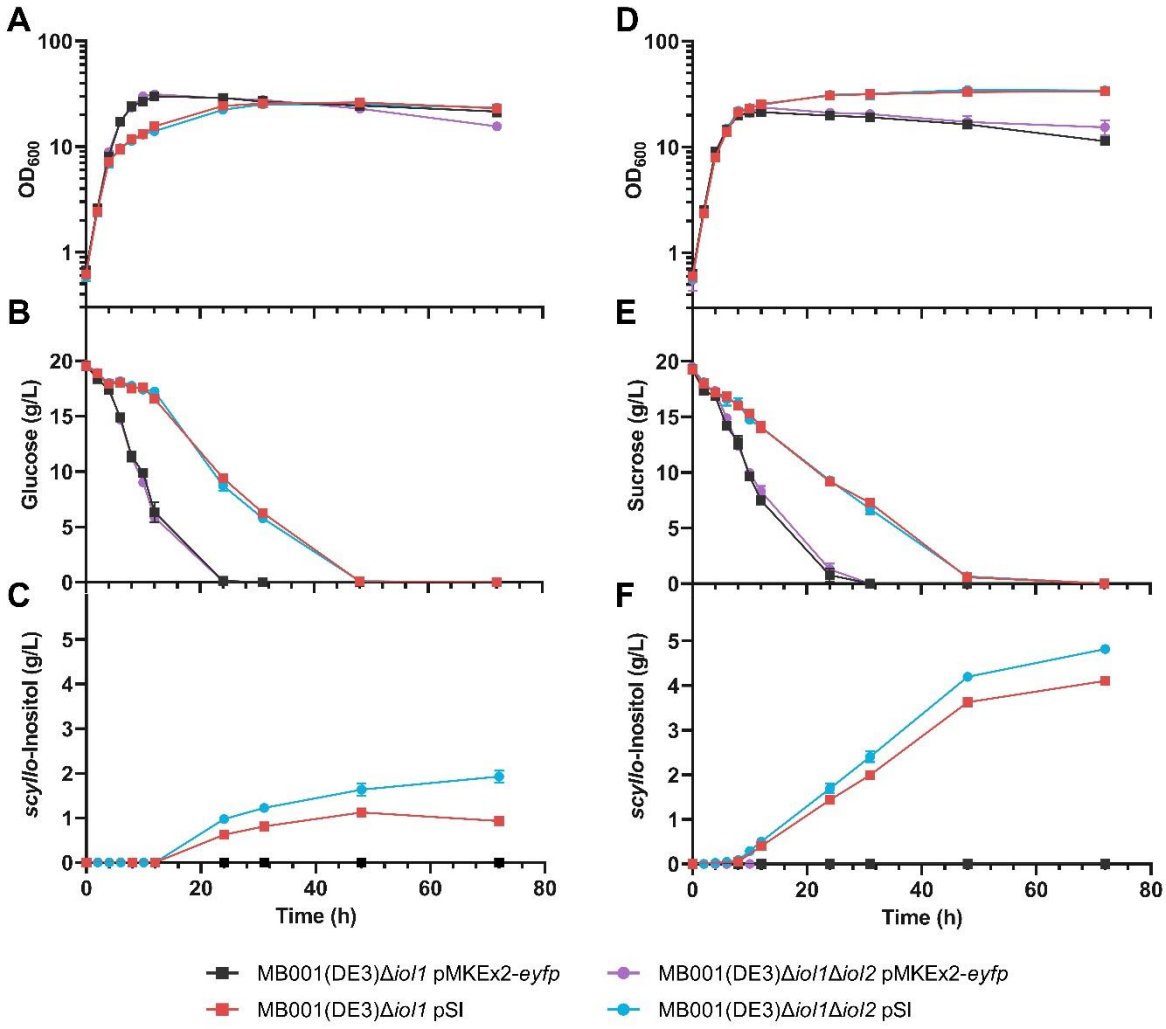

Fig. 6. Growth (A, D), glucose and sucrose consumption (B, E), and production of *scyllo*-inositol (C, F) of the indicated *C. glutamicum* strains during cultivation in BHI medium with 20 g/L glucose (A-C) or with 20 g/L sucrose (D-F). Target gene expression was induced at an OD_{600} of 2 with 200 µM IPTG. Mean values of three biological replicates and standard deviations are shown.

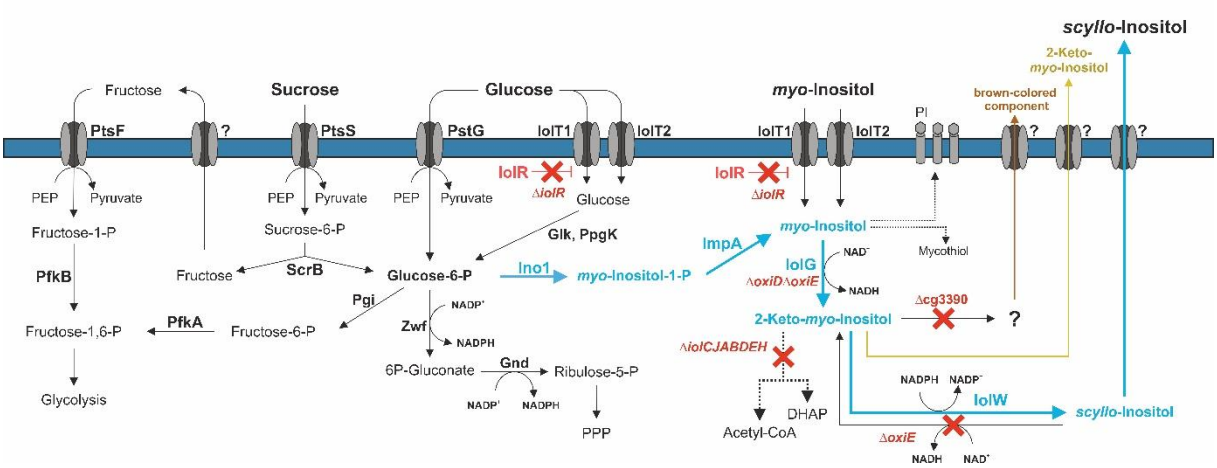

Fig. 7. Scheme of metabolism relevant for *scyllo*-inositol production from glucose, sucrose, and *myo*-inositol by *C. glutamicum*. The genes required for catabolizing of *myo*-inositol or catalyzing further conversions of inositol-derived metabolites (grey) and the gene encoding the transcriptional regulator IolR (red) were deleted in the strain MB001(DE3)Δ*iol1*Δ*iol2*. Highlighted in blue is the engineered pathway for *scyllo*-inositol production from either *myo*-inositol, glucose or sucrose employing *myo*-inositol 1-phosphate synthase (Ino1), *myo*-inositol 1-monophosphatase (ImpA), *myo*-inositol dehydrogenase (IolG), and *scyllo*-inositol dehydrogenase (IolW). IolT1 and IolT2: transporters for *myo*-inositol and glucose; PtsG, PtsF, PtsS: EII components of the PEP-dependent phosphotransferase system for uptake of glucose, fructose, and sucrose, respectively; PfkA: 6-phosphofructokinase; PfkB: 1-phosphofructokinase; ScrB: sucrose 6-phosphate hydrolase; Pgi: glucose 6-phosphate isomerase; Zwf: glucose 6-phosphate dehydrogenase; Gnd: 6-phosphogluconate dehydrogenase; Glk: glucokinase; PpgK: polyphosphate-dependent glucokinase; OxiD: enzyme with *myo*-inositol dehydrogenase activity; OxiE: enzyme with *scyllo*-inositol and *myo*-inositol dehydrogenase activity; Cg3390: enzyme converting 2-keto-*myo*-inositol to a yet unknown product responsible for brown coloration; PEP: phosphoenolpyruvate; DHAP: dihydroxyacetone phosphate; PI: phosphatidylinositol.

Supplementary information

Metabolic engineering of *Corynebacterium glutamicum* for production of *scyllo*-inositol, a drug candidate against Alzheimer's disease

Paul Ramp, Alexander Lehnert, Susanna Matamouros, Astrid Wirtz, Meike Baumgart, Michael Bott[#]

IBG-1: Biotechnology, Institute of Bio- and Geosciences, Forschungszentrum Jülich, Jülich, Germany

[#]Corresponding author: m.bott@fz-juelich.de

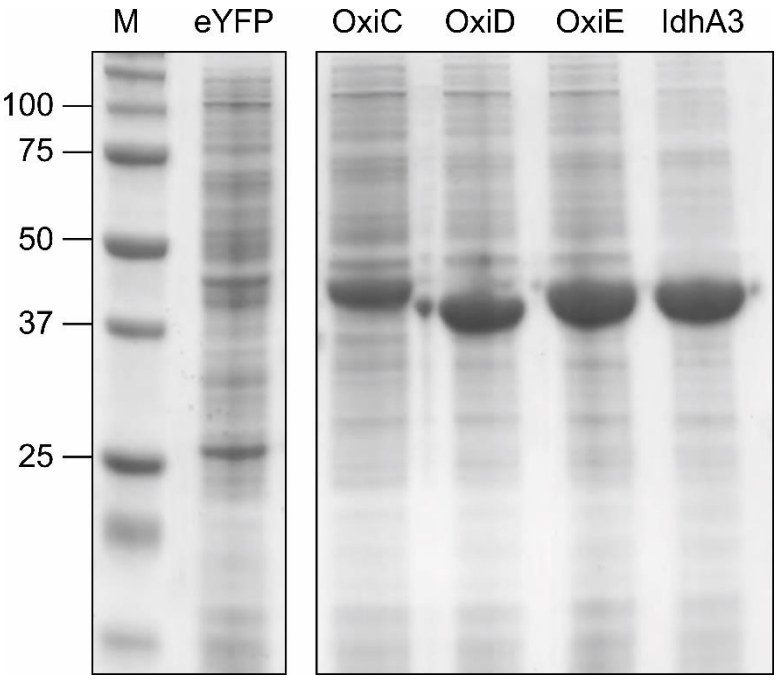

Fig. S1. Coomassie-stained SDS-polyacrylamide gel showing the overproduction of the *C. glutamicum* proteins OxiC (Cg3389, 39.58 kDa), OxiD (Cg3391, 36.23 kDa), OxiE (Cg3392, 38.03 kDa) and IdhA3 (Cg2313, 35.21 kDa). The proteins were overexpressed with the vector pMKEx2 in the *C. glutamicum* strain MB001(DE3)Δ*iol1*Δ*iol2* as described in the Methods section. Cell-free extracts of the different strains were prepared and 10 µg protein were separated by SDS-PAGE. M, marker proteins with molecular masses indicated in kDa.